Title

Isolation and characterization of a Halomonas species for non-axenic growth-associated production of bio-polyesters from sustainable feedstocks.

Journal

Applied and Environmental Microbiology, 90(8)

Authors

Woo, Sung-Geun

Averesch, Nils

Berliner, Aaron

et al.

Publication Date

2024-08-21

DOI

10.1128/aem.00603-24

AMERICAN SOCIETY FOR MICROBIOLOGY | Applied and Environmental Microbiology

Check for updates

| Applied and Industrial Microbiology | Full-Length Text

Isolation and characterization of a *Halomonas* species for non-axenic growth-associated production of bio-polyesters from sustainable feedstocks

Sung-Geun Woo,[1,2] Nils J. H. Averesch,[1,2] Aaron J. Berliner,[1,3] Joerg S. Deutzmann,[2] Vince E. Pane,[1,4] Sulogna Chatterjee,[1,2] Craig S. Criddle[1,2]

AUTHOR AFFILIATIONS See affiliation list on p. 19.

ABSTRACT Biodegradable plastics are urgently needed to replace petroleum-derived polymeric materials and prevent their accumulation in the environment. To this end, we isolated and characterized a halophilic and alkaliphilic bacterium from the Great Salt Lake in Utah. The isolate was identified as a *Halomonas* species and designated "CUBES01." Full-genome sequencing and genomic reconstruction revealed the unique genetic traits and metabolic capabilities of the strain, including the common polyhydroxyalkanoate (PHA) biosynthesis pathway. Fluorescence staining identified intracellular polyester granules that accumulated predominantly during the strain's exponential growth, a feature rarely found among natural PHA producers. CUBES01 was found to metabolize a range of renewable carbon feedstocks, including glucosamine and acetyl-glucosamine, as well as sucrose, glucose, fructose, and further glycerol, propionate, and acetate. Depending on the substrate, the strain accumulated up to ~60% of its biomass (dry wt/wt) in poly(3-hydroxybutyrate), while reaching a doubling time of 1.7 h at 30°C and an optimum osmolarity of 1 M sodium chloride and a pH of 8.8. The physiological preferences of the strain may not only enable long-term aseptic cultivation but also facilitate the release of intracellular products through osmolysis. The development of a minimal medium also allowed the estimation of maximum polyhydroxybutyrate production rates, which were projected to exceed 5 g/h. Finally, also, the genetic tractability of the strain was assessed in conjugation experiments: two orthogonal plasmid vectors were stable in the heterologous host, thereby opening the possibility of genetic engineering through the introduction of foreign genes.

IMPORTANCE The urgent need for renewable replacements for synthetic materials may be addressed through microbial biotechnology. To simplify the large-scale implementation of such bio-processes, robust cell factories that can utilize sustainable and widely available feedstocks are pivotal. To this end, non-axenic growth-associated production could reduce operational costs and enhance biomass productivity, thereby improving commercial competitiveness. Another major cost factor is downstream processing, especially in the case of intracellular products, such as bio-polyesters. Simplified cell-lysis strategies could also further improve economic viability.

KEYWORDS Great Salt Lake, extremophile, halophile, *Halomonas*, full-genome sequencing, bioplastic, polyester, genetic engineering

Earth's biosphere and all lives within are being threatened by an unprecedented accumulation of synthetic materials of anthropogenic origin, commonly known as plastics (1–3). In the US, plastics make up about 12% of municipal solid waste (4). The global production of petroleum-based plastics reached 391 MMt/a in 2021; projected

Editor John R. Spear, Colorado School of Mines, Golden, Colorado, USA

Address correspondence to Sung-Geun Woo, wsg135@stanford.edu, or Nils J. H. Averesch, nils.averesch@uq.net.au.

Sung-Geun Woo and Nils J. H. Averesch contributed equally to this article. Author order was determined by prior agreement and verified throughout the writing process.

The authors declare no conflict of interest.

See the funding table on p. 20.

Received 27 March 2024
Accepted 20 June 2024
Published 26 July 2024

to grow exponentially for the foreseeable future, it will soon surpass a volume of half a gigaton per year (5). Currently, the US' plastics industry alone accounts for 3.2 quadrillion BTU (quads) of annual energy use, resulting in over 100 Mmt CO_2e/a of greenhouse gas (GHG) emissions (2).

Both, the contribution to global warming from the production of synthetic materials and the contamination of the biosphere at their end-of-life, have aggravated environmental problems with consequences on a global scale: the damage inflicted on the economy likely exceeds the revenue generated by the plastics manufacturing industry (6, 7). Therefore, renewable and readily deconstructable materials are urgently needed. Hence, efforts to recycle and reuse waste streams into renewable materials are being boosted. This includes the upcycling of spent plastics and/or their synthesis from GHGs. Complementing catalytic methods, many approaches now rely upon biotechnology, employing a variety of plants, algae, fungi, or microorganisms (8–13).

Biological polyesters, such as polyhydroxyalkanoates (PHAs), can be derived from recovered carbon feedstocks and are promising polymers for utilization as renewable and biodegradable thermoplastics. The most common PHA is polyhydroxybutyrate (PHB), which has material properties similar to poly(lactic acid) and can be fabricated into diverse plastic products (14–19). The commercial success of PHAs has, however, been hampered by their production costs that still exceed the price of petrochemistry-derived plastics (which often cost less than $2/kg) by two- to fourfold (9, 20). The operational expenses (OpEx) of a biotechnological process are strongly influenced by the performance parameters of the employed microorganism in terms of rate, titer, and yield. While volumetric production rates of PHB exceeding 2 $g_{PHB}/(L \times h)$, cell densities higher than 100 g/L, and per-biomass yields of over 90% (wt/wt) have been reached (9, 21), the effective productivity of bio-polyesters often falls short of the theoretical maxima, primarily because they are typically synthesized only toward the end of the growth cycle. [The accumulation of PHAs is commonly triggered by stress and/or nutrient limitation (22).] In addition, extensive cleaning and sterilization of cultivation vessels between batches result in significant downtime, and maintaining pure cultures demands sterile conditions throughout the run. This can significantly increase the OpEx of a process. Further, techno-economic analyses have revealed that the feedstock can constitute up to 50% of the overall production cost, in case common substrates such as refined sugars, noble oils, or fatty acids are used. Downstream purification of PHAs from biomass commonly involves solvent-based lysis and separation steps, adding to costs: extraction employing halogenated solvents can account for 20%–25% of overall expenses (20).

Aseptic conditions can be maintained much more easily with extremophiles as cultures thereof can be kept axenic in non-sterile environments (23). In particular, halophiles have already been employed for the production of bioplastics in several instances (21, 24). Especially *Halomonadaceae* have recently experienced an onslaught of exploration for the production of PHAs. For example, the species *Halomonas bluephagenesis* is well characterized and among the highest producers: the wild type accumulates as much as 84% (wt/wt) of its cell dry weight (CDW) in PHB, which has been driven up to 94% (wt/wt) through metabolic engineering (25). Further, polyesters can be released from the cells of halophiles through osmolysis, partially abolishing the need for solvents (26), which can save additional costs.

Presumably, halophilic microorganisms produce osmolytes to ward themselves from hypersaline environments (27–31). PHB has been suggested to serve as an agent against protein aggregation; it is also known that enhanced salt tolerance in microbes can lead to increased PHB production (32, 33). Motivated by that, the Great Salt Lake (GSL) in Utah, a large body of water with extremely high salinity, was chosen as a promising location to isolate a microbe that could be domesticated and employed for the low-cost production of PHB.

RESULTS

Isolation and basic characterization of a halophilic microbe

A water sample was taken from the north arm (Gunnison Bay) of the GSL (Shoshone: *Ti'tsa-pa*), as shown in Fig. 1a, from which microbes were enriched and selected for halophily under extreme osmolarity (3.4 M sodium chloride $\triangleq$ 6.8 osmol/L). Six isolates were obtained at 30°C on a complex substrate, all of which belonged to the same species based on their 16S rRNA sequences (OQ359097.1). The closest relative was *Halomonas gomseomensis* M12 (NR042488.1), with ~99.7% 16S rRNA gene identity. The hitherto undescribed *Halomonas* strain was designated "CUBES01" and exhibited a maximum growth rate of 0.402 h^{-1} on a complex substrate (Fig. 1c); Nile red staining and fluorescence microscopy revealed the presence of intracellular granules (Fig. 1b), which were indicative of poly(3-hydroxybutyrate) biosynthesis.

Phylogenetic classification of the *Halomonas* isolate

The phylogenetic analysis of *Halomonas* sp. CUBES01 was conducted based on its 16S rRNA gene sequence. Within a phylogenetic tree of 50 *Halomonas* 16S RNA sequences (Fig. 2), strain CUBES01 clustered together with *H. gomseomensis* M12 into a single branch. *Halomonas arcis* AJ282, *Halomonas azerica* TBZ9, *Halomonas janggokensis* M24, and *Halomonas subterranea* ZG16 formed the closest neighboring group to CUBES01 and *H. gomseomensis*. The pairwise genetic distance heatmap in Fig. 3 supports the phylogenetic analysis. Specifically, *H. gomseomensis* M12 (99.7%), *H. arcis* AJ282 (98.2%), *H. subterranea* ZG16 (97.8%), and *H. janggokensis* M24 (97.7%) exhibited high 16S rRNA sequence identity. Other *Halomonas* strains exhibited a genetic identity ranging from 95.2% to 97.7%, with the exception of *Halomonas lysinitropha* 3(2) which at 93.7% similarity was more distantly related.

The profiles of fatty acids and respiratory quinones of *Halomonas* sp. CUBES01 were consistent with the relationships observed in the pairwise genetic analysis: the predominant fatty acid, $C_{18:1}$ ω7c, constituted 54.9% of the profile (see Table S1 for full composition); the strongly predominant ubiquinone of *Halomonas* sp. CUBES01 was Co-Q9 (97.5%), followed by Co-Q8 (1.2%) and Co-Q10 (1.3%).

Genotypic characterization of the *Halomonas* isolate

Full-genome sequencing and genomic reconstruction of *Halomonas* sp. CUBES01 revealed a single circular chromosome of 3,642 kbp with a G+C content of 60.1% (Fig. 4).

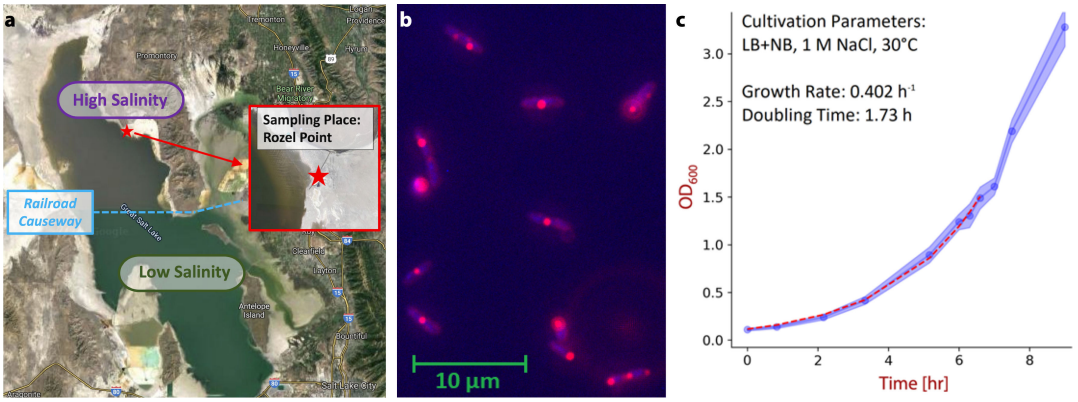

FIG 1 Isolation and initial characterization of *Halomonas* species. (a) Point of sample collection, marked on a map of the Great Salt Lake, UT, USA. Specifically, samples were taken off the Spiral Jetty near Rozel Point at coordinates 41°26′15.5″N 112°40′09.7″W. Imagery ©2024 Terra Metrics, Map data ©2024 Google. (b) Microscopy of *Halomonas* species with fluorescence staining of intracellular polyester granules. (c) Growth curve of isolated *Halomonas* species on rich complex medium (aerobic, 30°C, 1 M NaCl).

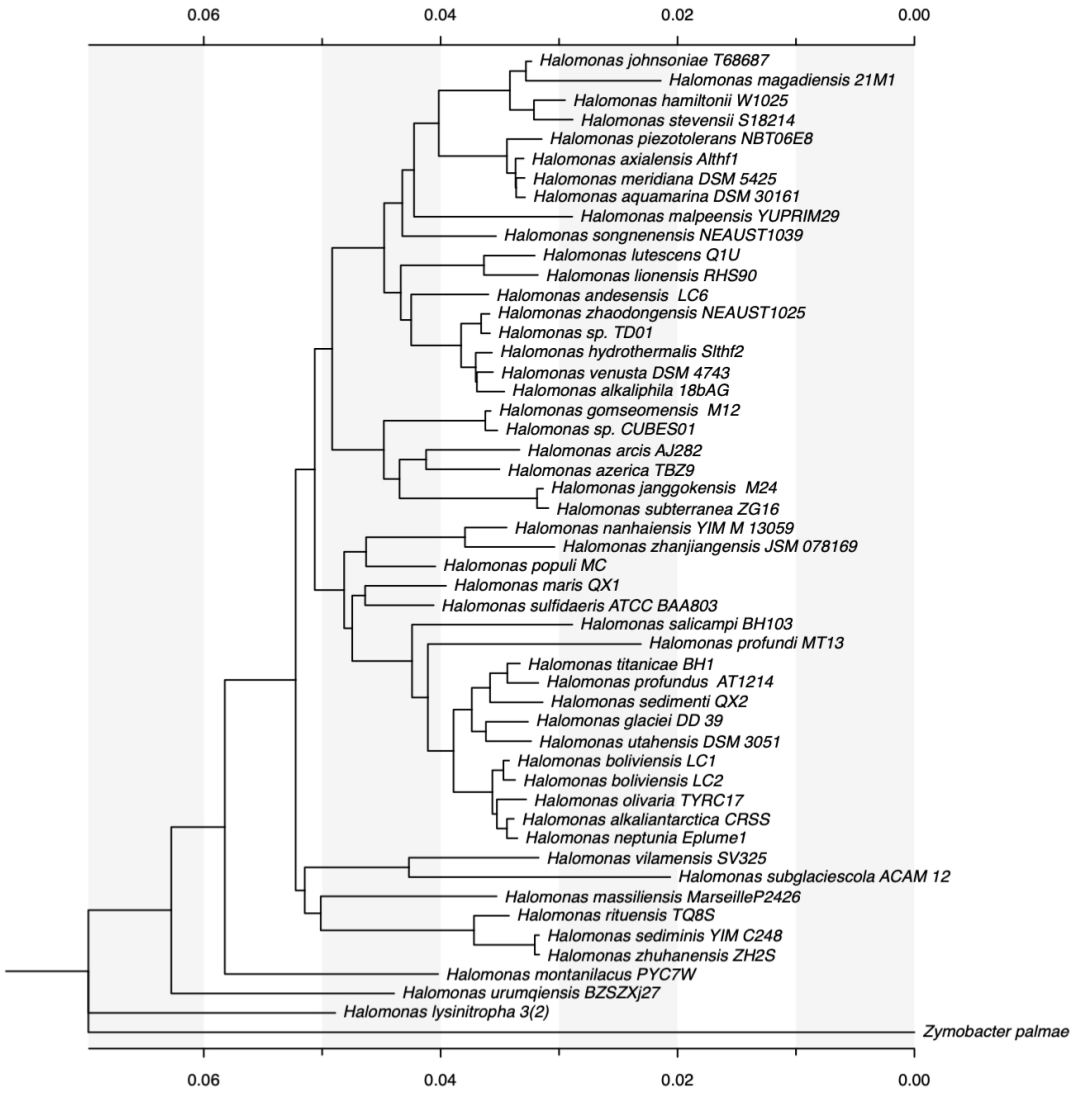

FIG 2 Phylogenetic affiliation and neighborhood of *Halomonas* sp. CUBES01 based on 16S rRNA sequence comparison in the form of a phylogenetic tree based on the minimum evolution method.

Genome features

Biological functions were assigned to 3,095 of the 3,396 predicted coding sequences (Table 1). The remaining 301 coding sequences comprised one conserved hypothetical protein and 300 hypothetical proteins of unknown function. Preliminary analysis of the assembled genome with Pathway Tools revealed 6,792 genes, 345 pathways, 2,001 enzymatic reactions, 130 transport reactions, 230 protein complexes, 2,193 enzymes, 684 transporters, 1,369 compounds, 4,786 transcription units, and 575 GO terms. In addition, the codon usage bias (CUB) of *H*. sp. CUBES01 was determined based on the assembled genome files (contigs 1 and 2) identified from the sequenced genome (see Fig. S1).

Metabolic features

All central metabolic pathways common among heterotrophic bacteria were annotated for *Halomonas* sp. CUBES01; a count of the major metabolic functions distinguished into 30 categories can be found in Fig. S2. The genome analysis revealed the genetic basis for core catabolic capabilities, such as the uptake and breakdown of various sugars and carbonic acids and complex anabolic capabilities of potential biotechnological interest.

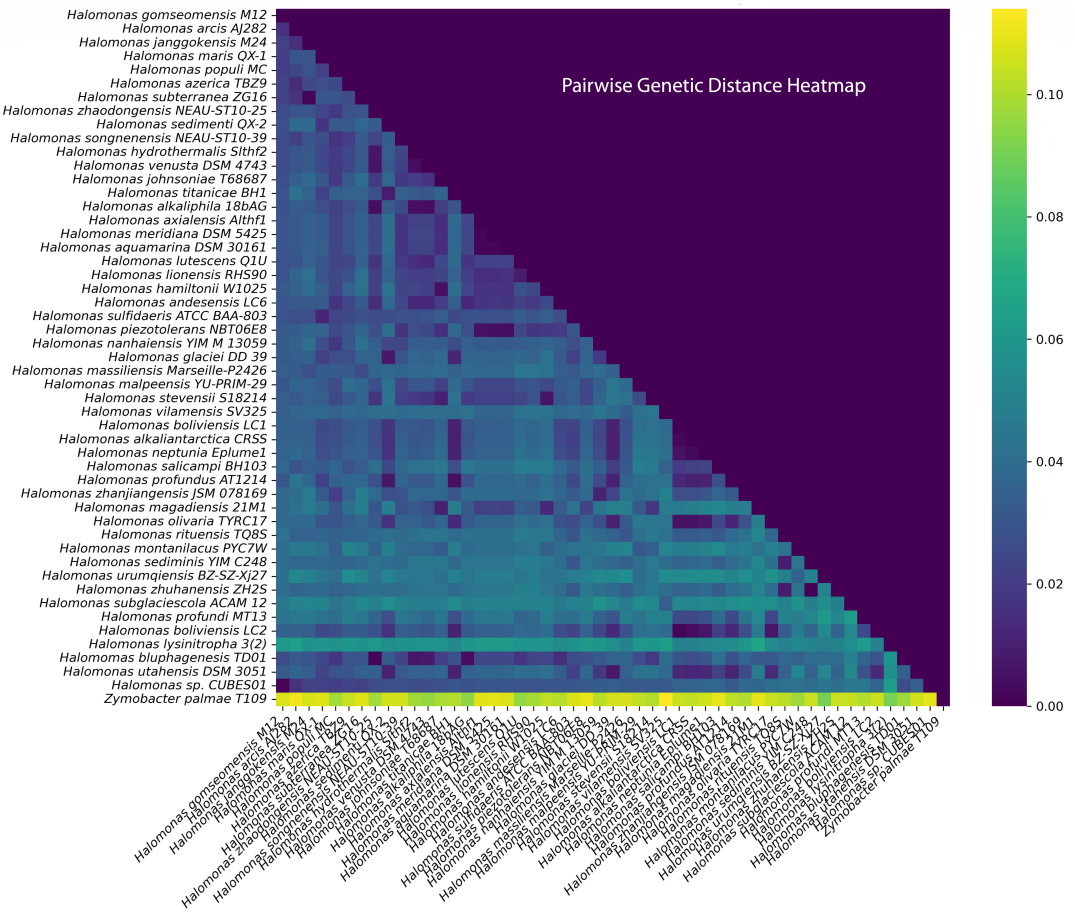

FIG 3 Phylogenetic affiliation and neighborhood of *Halomonas* sp. CUBES01 based on 16S rRNA sequence comparison in the form of a heatmap of the pairwise 16S rRNA gene sequence distance of CUBES01 to other strains. The scale indicates the fraction of non-identical base pairs between the compared sequences. GenBank IDs for each *Halomonas* species can be found in Table S7.

Certain metabolic features of particular interest are highlighted in the following. A complete overview of all metabolic capabilities of *Halomonas* sp. CUBES01 is provided in the form of a metabolic map in SI1.

Species of the *Halomonas* genus are well known for their capacity to accumulate PHB (21). In CUBES01, 17 genes associated with PHA synthesis were identified. Among these, three *phaA*, one *phaB*, two *phaC*, and one *phaZ* genes were annotated, encoding *β*-ketothiolase (acetyl-CoA acetyltransferase), acetoacetyl-CoA reductase, PHA synthase, and PHA depolymerase, respectively. Notably, *phaA1* (MEC4767736.1), *phaA2* (MEC4768916.1), *phaA3* (MEC4766063.1), *phaB* (MEC4766145.1), *phaC1* (MEC4767859.1), and *phaC2* (MEC4767548.1) were not organized in common operons but dispersed throughout the genome. Of the PHA synthase genes, *phaC1* belonged to class I, but *phaC2* could not be assigned to any known class (*phaC1* encoded 617 and *phaC2* 794 amino acids, corresponding to expected molecular weights of 70 and 89 kDa, respectively). While the two PHA synthases are, therefore, not classic isozymes, both still exhibit the conserved catalytic triad (Cys-Asp-His) (21, 34). Additionally, PHA metabolism also encompassed regulator genes such as *phaP* (MEC4767860.1) and *phaR* (MEC4766665.1) that are associated with phasin formation and PHA synthesis autoregulation, respectively, as well as one *phaZ* (MEC4768861.1) of PHA depolymerization.

The genome of CUBES01 also harbored genes of the major biosynthesis pathway of ectoine, comprised of *ectA* (MEC4767328.1), *ectB* (MEC4767329.1), *ectC* (MEC4767330.1), and *ectD* (MEC4766129.1), encoding for L-2,4-diaminobutyric acid acetyltransferase,

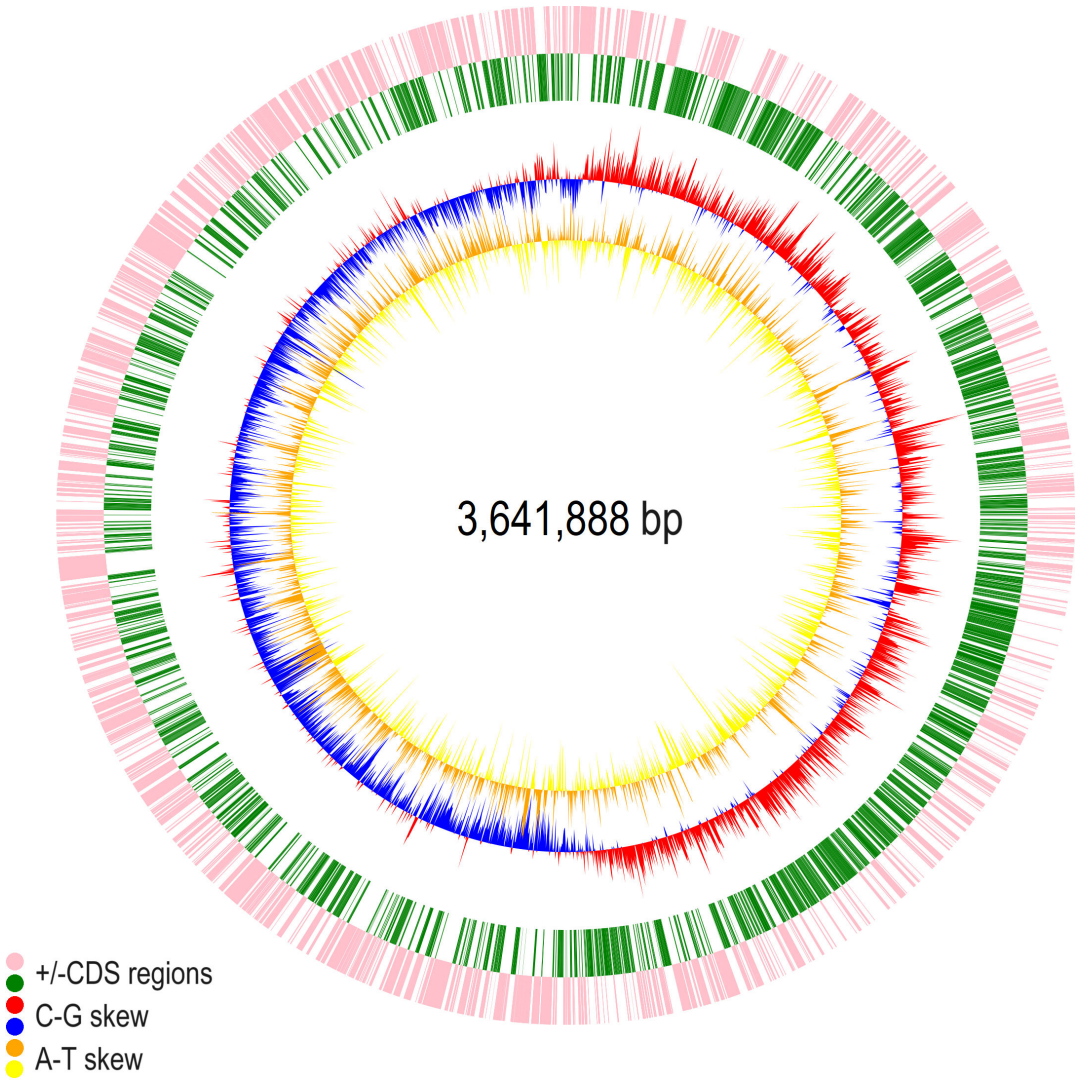

FIG 4 Circular representations of the *Halomonas* sp. CUBES01 chromosome displaying relevant genome features; yellow/orange: A-T skew; blue/red: C-G skew; green: +CDS regions; pink: −CDS regions.

L-2,4-diaminobutyric acid transaminase, ectoine synthase, and ectoine hydroxylase, respectively (30).

The genome of CUBES01 further contained genes associated with DABs (35) on contig 1 (MEC4768999.1 and MEC4768998.1) and contig 2 (MEC4769013.1). The DAB operon, consisting of *dabA* (PFAM: PF10070) and *dabB* (PFAM: PF00361), encodes an energy-coupled inorganic carbon (C_i) pump (36), presumably assuming the function of a hydrophilic protein that establishes chemical equilibrium between CO_2 and HCO_3^-. Notably, the genome of CUBES01 contains one copy each of *dabA* (MEC4768999.1) and *dabB* (MEC4768998.1) genes co-located within contig 1, while another *dabA* gene (MEC4769013.1) was found within contig 2.

Phenotypic characterization of the *Halomonas* isolate

Boundary conditions for the cultivation of *Halomonas* sp. CUBES01 were established, enabling a more specific phenotypic characterization of the strain.

TABLE 1 Features of the *Halomonas* sp. CUBES01 genome and coding sequences

Feature	Contig 1	Contig 2
Size (bp)	3,641,888	26,118
Fraction of genome coding (%)	90.41	92.79
Coding sequences (#)	3,373	23
Function assigned (#)	3,073	22
Hypothetical proteins (#)	300	0
Conserved hypothetical proteins (#)	1	0
Average ORF length (bp)	976.12	1,053.65
Maximal ORF length (bp)	11,895	2,379
GC content (%)	60.0	60.7
ATG initiation codons (%)	87.67	82.6
GTG initiation codons (%)	9.07	8.7
TTG initiation codons (%)	3.2	0.0

Basic cultivation conditions

Halomonas sp. CUBES01 exhibited growth only under conditions of substantial osmolarity: on nutrient broth (NB) agar, biomass formed overnight at sodium chloride concentrations between 40 and 100 g/L; the lowest sodium chloride concentration enabling growth was 30 g/L (Fig. S3). At 200 g/L sodium chloride, the formation of biomass only occurred after 2 weeks of incubation at 30°C on liquid NB. Optimum growth was observed between 60 and 80 g/L sodium chloride (Fig. S3), making CUBES01 a moderate halophile (37, 38). Hence, 1 M sodium chloride was used routinely to provide optimum growth conditions (58 g/L; osmotic pressure of ~0.3 MPa). Optimum growth was observed at 30°C (growth slowed at room temperature and stagnated at 37°C). The viable pH range of strain CUBES01 was determined to be between pH 7.2 and pH 9.8, with an optimum at pH 8.8 (Fig. S4). CUBES01 can, therefore, also be characterized as alkaliphilic. Using the established optimum cultivation conditions (1 M sodium chloride and pH 8.8), the maximum doubling time during aerobic growth at 30°C was determined as ~1.7 h (on complex medium, Fig. 1c).

Substrate spectrum

The *Halomonas* strain was further characterized by its ability to utilize different carbon sources as substrates. For this purpose, a chemically defined medium was developed (Table 2). Specifically, a combination of phosphate and carbonate buffer was used to maintain alkalinity while sodium chloride upheld the required ionic strength. With potassium nitrate serving as a source of nitrogen, CUBES01 was found to accept sucrose, glucose, fructose, and glycerol, as well as acetate, as a carbon and energy source; in the absence of inorganic fixed nitrogen, the amino sugars glucosamine and acetyl-glucosamine served as the sole carbon and nitrogen source. The highest growth rates and biomass concentrations were observed with sucrose and glucose (0.17^{-1} and 0.15^{-1}, respectively). The amino sugars also enabled high cell density, albeit formed at a much

TABLE 2 Main components of chemically defined medium

Component	Volume (mL/L)	Comments/Notes
Basic salts (10×)	500	
Trace elements (1,000×)	1	
Phosphate buffer (50×, 4 mM final)	20	
Carbonate buffer (25×, 40 mM final)	40	Phosphate and carbonate solutions should be prepared separately
Carbon source	Variable	Required volume depends on the stock solution and desired final concentration (e.g., 10 or 20 g/L)
Water	Variable	Up to a final volume of 1 L

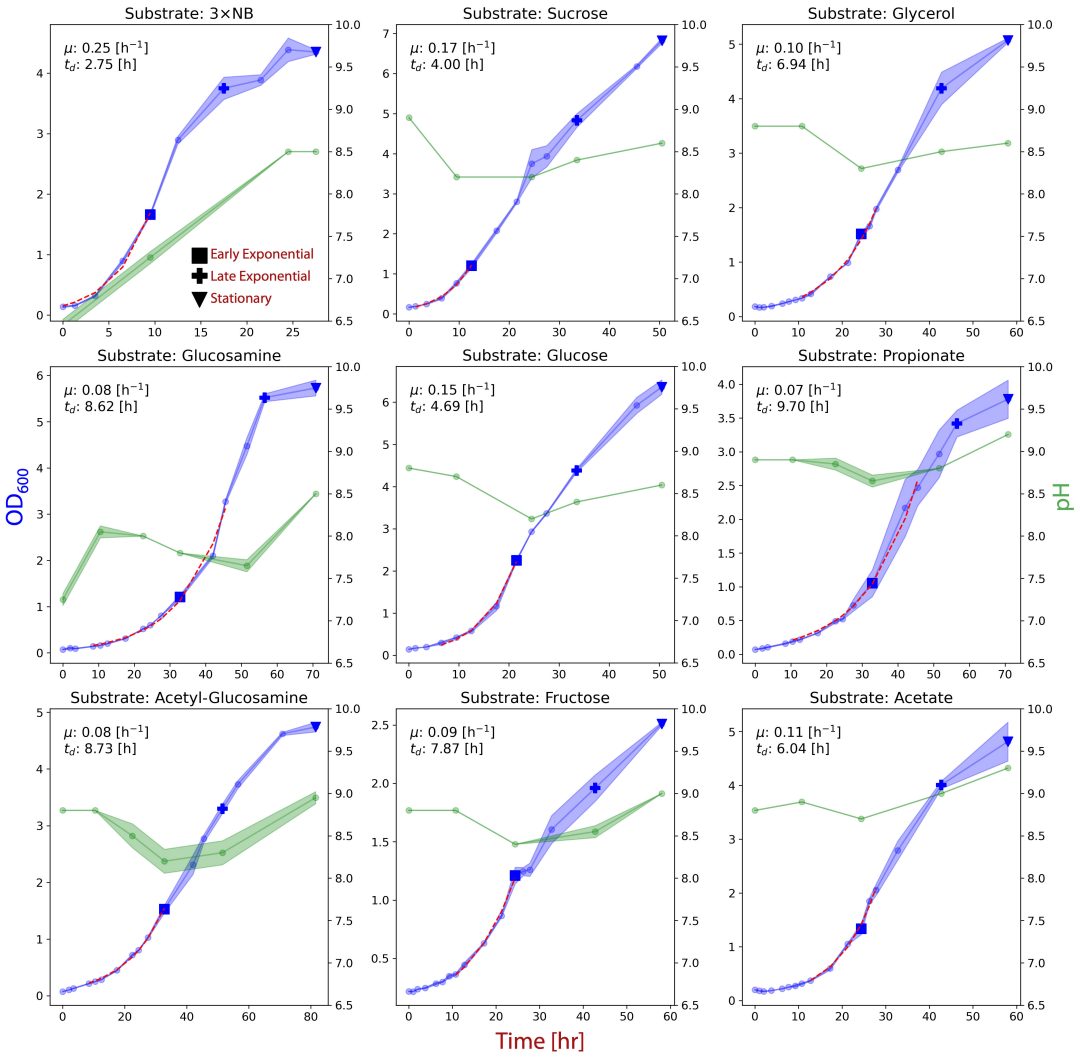

FIG 5 Growth of *Halomonas* sp. CUBES01 on different substrates (equivalent C-mol quantities of all substrates except for NB). The blue graphs represent the growth curves while the green graphs represent the pH throughout the cultivation. The exponential phases used to calculate growth rates are indicated by red dashed lines. Sampling points for quantification of PHB content are represented by square (early exponential), cross (late exponential), and triangle (stationary) symbols and directly correspond to the data shown in Fig. 6. The same sampling points were also used for end-product analysis.

slower rate (Fig. 5). The lowest cell density was obtained on fructose followed by growth on propionate. The growth rates on acetate and glycerol exceeded those on the amino sugars, but the final biomass was slightly lower. An analytical profile index 50 CH test further revealed the ability of the strain to utilize arabinose, galactose, maltose, mannitol, and trehalose by CUBES01 (Table S2).

Products

Using solvent extraction, polyesters can be solubilized and separated from the biomass of PHA-producing microbes (39). Applying chloroform to dried biomass of *Halomonas* sp. CUBES01, a resin was obtained that resembled a thermoplastic material when dried. Nuclear magnetic resonance (NMR) spectroscopy (Fig. S5a) confirmed that the extracted compound was a polyester; specifically, the sextet resonance at a chemical shift of 5.25 ppm in the ^{1}H-NMR spectrum was indicative of poly(3-hydroxybutyrate). Gel permeation chromatography (GPC) (Fig. S5b) determined the weight- and number-average molecular weights (M_w and M_n) and polydispersity index of the polymer, which were on the order of 572 and 341 kDa and 1.67, respectively.

Furthermore, high-performance liquid chromatography (HPLC) revealed the accumulation of acetate and lactate in supernatants of CUBES01 when cultivated on sugars as in the experiments underlying Fig. 5.

Microscopy and morphology

While distinctively separated from each other (not adhering), live cells of *Halomonas* sp. CUBES01 appeared rod-shaped and motile, measuring approx. 1–4 µm long and 0.8–1 µm wide. Stained with Nile red, fluorescence microscopy revealed the count/size of intracellular inclusion bodies, which was highest/greatest during the exponential growth phase (see Fig. S6a and b as well as SI2 for microscopy images of samples collected at different time points during the cultivation of CUBES01 on chemically defined medium as per Fig. 5).

Antibiotic sensitivity and transformability

Halomonas sp. CUBES01 was found to be sensitive to 43 of the 44 tested antibiotics (see Tables S3 and S4). Among these were ampicillin, carbenicillin, kanamycin, neomycin, gentamicin, tetracycline, erythromycin, streptomycin, spectinomycin, and chloramphenicol, which are commonly used as selection markers for plasmid maintenance in shuttle vector systems (40).

Furthermore, to assess the strain's genetic tractability, a protocol for the transformation of CUBES01 through bacterial conjugation was developed. Especially CUBES01's strict requirement for halophilic conditions proved challenging, since common *Escherichia coli* donor strains hardly tolerated more than 40 g/L of sodium chloride. Nevertheless, at 35 g/L of sodium chloride, the growth of both species was sufficient to allow for adequate conjugation efficiency, yielding ~100 and ~1,000 colonies per plate, respectively, depending on the employed plasmid vector (Fig. S7). The difference is attributed to the unique genetic traits thereof but may have also been influenced by the amount of biomass recovered after conjugation, as well as the dilution factor of the cell suspension when selecting exconjugants for antibiotic resistance to obtain transconjugants.

Specifically, three different broad-host-range plasmids based on either the RP4 (RK2) or the pBBR1 conjugative system were tested (pTJS140, pBBR1MCS, and pCM66T; see Table S5 for details). As was evident from the overnight growth of the transformed mutants on antibiotic-containing agar plates, CUBES01 accepted the respective RK2/RP4 and pBBR1 plasmids pTJS140 and pBBR1MCS, selectable on Strep^R/Spec^R and Kan^R/Neo^R, well. The Kan^R/Neo^R selectable RK2/RP4 plasmid pCM66T appeared to be difficult to maintain by CUBES01, as the colony formation of transformed mutants required several days of incubation on selective medium. Using PCR-based verification methods, full coverage for the plasmids pTJS140 and pBBR1MCS was obtained in over 90% of the isolated exconjugants (Fig. S8), verifying the circularity of the vectors and confirming the antibiotic-resistant mutants of CUBES01 as transconjugants. Additionally, genetic material obtained from the cultivated *Halomonas* mutants was used to transform competent *E. coli*, validating their genetic integrity (i.e., no re-arrangement of the heterologous DNA) and providing a strong indication for the maintenance of self-replicating shuttle vectors' conformation (i.e., no genomic integration of the heterologous DNA).

Employing the *Halomonas* isolate for bio-polyester production

Isolated with the intent to be employed for sustainable bio-polyester production, the capacity of *Halomonas* sp. CUBES01 to accumulate PHB and the applicability of simplified downstream processing techniques for the release of the intracellular product were investigated.

Formation of PHB on different substrates

To further characterize the capacity of CUBES01 to form bio-polyesters, the per-biomass PHB content obtained from the cultivation of the strain on different feedstocks was assessed. Determination of the relative (normalized to biomass concentration) fluorescence intensity of cell culture stained with Nile red allowed consistent qualitative assessment of PHB production at different growth stages: on NB, the accumulation of bio-polyesters appeared to be the highest in the early exponential phase, while on minimal medium, the highest signal intensity was observed in the late exponential phase for most substrates (except in the case of glucose or propionate as carbon sources), as evident from Fig. 6. The highest PHB content from gravimetric quantification after extractive purification of the bio-polyesters from biomass samples was obtained when CUBES01 was supplied with acetate, glycerol, or sucrose as substrates [69 ± 8%, 79 ± 8%, and 55 ± 31% ($g_{PHB}/g_{biomass}$), respectively, as per Fig. 6].

Release of PHB through osmolysis

When exposing cells of CUBES01 to deionized water, the initial OD of 0.6 dropped almost immediately to 0.1 (Fig. S9a), indicating efficient and rapid lysis. Complete lysis was confirmed by the absence of colony-forming units (CFU) when dilutions of cells exposed to deionized water were plated on a solid growth medium (in contrast to hundreds of colonies for the untreated culture, see Fig. S9b).

DISCUSSION

Phylogeny

The phylogenetic tree and the pairwise distance comparisons of 16S rRNA sequences (Fig. 2 and 3) both identified *H. gomseomensis* as the closest relative of CUBES01. Analysis of the cellular fatty acid composition verified the close phylogenetic relationship between CUBES01 and *H. gomseomensis* M12 and also *H. janggokensis* M24, which were both isolated from solar salterns in South Korea (41), and *H. lutescens* Q1T, isolated from Qinghai Lake, China (42). Given that C16:0 was the predominant fatty acid in the profiles of *H. lysinitropha* 3(2), isolated from the Meighan Wetland, Iran, and *Halomonas* sp.

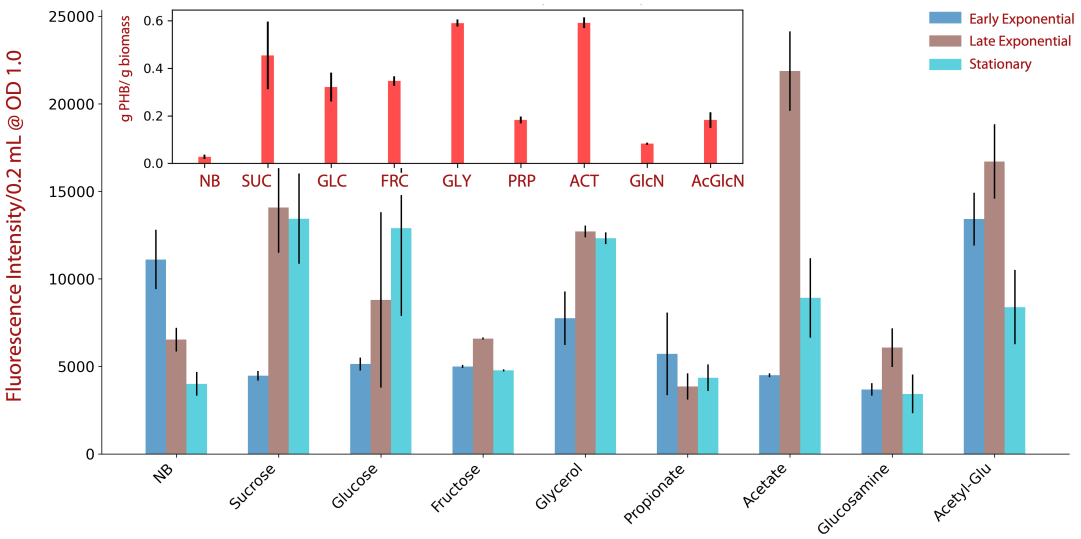

FIG 6 Accumulation of PHB by *Halomonas* sp. CUBES01 in early exponential (blue), late exponential (ochre), and stationary (turquoise) growth phase on different substrates, directly corresponding to the sampling points indicated in Fig. 5. While the main chart reflects the qualitative PHB content dependent on the growth stage [inferred by fluorescence intensity of whole cells stained with Nile red and normalized to optical density (OD)], the inset indicates the quantitative per-biomass PHB yield (obtained gravimetrically, late exponential and stationary phase combined). SUC, sucrose; GLC, glucose; FRC, fructose; GLY, glycerol; PRP, propionate; ACT, acetate; GlcN, glucosamine; AcGlcN, acetyl-glucosamine.

NA10-65 from the GSL, Utah (43, 44), the greater phylogenetic distance of CUBES01 from these strains is fitting. Also, the respiratory quinone pattern of CUBES01's was consistent with those reported for *H. gomseomensis* M12, *H. janggokensis* M24, *H. lysinitropha* 3(2), and *H. lutescens* Q1U (41, 42, 44).

Metabolism

While CUBES01 possesses all common genetic traits of PHA metabolism comprising the biosynthetic genes *phaA*, *phaB*, and *phaC*, as well as the regulatory genes *phaR* and *phaP*, they are scattered throughout the genome: the three major genes of PHA biosynthesis are not co-located in the common *phaABC* operon; only *phaP* and *phaC1* are adjacent. Common among PHA producers, this co-location often occurs within an interval of 5–211 nucleotides between the two genes (45); in the case of CUBES01, the distance is 112 nucleotides. In several *Halomonadaceae,* the latter is often located downstream of the former [i.e., *phaP-phaC*, in contrast to the common organization of the PHA biosynthetic locus (46)]. The coordinating role of PhaP, a so-called phasin, has been recognized previously (47): by interacting with the N-terminal domain of PhaC, it stabilizes the elongation of the polymer chain and, thus, defines the size of the PHB granule. Of the two PHA synthases, PhaC1 is fairly common; PhaC2 is less common; however, homologs thereof, which have a longer C- and shorter N-terminal domain, are still frequent in several *Halomonadaceae*, such as the species *bluephagenesis* TD01 (45). The absence of *phaP* adjacent to the *phaC2* gene on the genome of CUBES01 in combination with the shorter N-terminal domain of that enzyme could mean that (i) PhaP is not co-expressed with PhaC2 and (ii) no interaction on the protein level is possible. This could be an indication of this PHA synthase's constitutive expression. Also, PhaR, a repressor and autoregulator of PHA biosynthesis (46), was identified in CUBES01. In well-studied PHA producers, such as *Cupriavidus necator* and *Haloferax mediterranei*, PhaR is usually found close to the PHA synthetic locus and negatively regulates it, influencing PhaP expression in dependence on the abundance and maturity of PHB granules (48, 49). In CUBES01, *phaR* is not located in the vicinity of any of the other PHA-regulatory or -biosynthetic genes. While the specific functions and interactions of PhaP and PhaR with each other as well as PHB in *Halomonas* CUBES01 remain elusive, the significant differences in the genomic organization of these genes suggest a substantially different regulation of PHA metabolism. The fact that *phaA* and *phaB* are also not co-located with either of the *phaC*s nor *phaR* and *phaP* suggests their independent regulation, which could explain the observed perpetual PHB production.

The *dabA* genes code for a protein subunit with a domain homologous to *β*-carbonic anhydrases, which is crucial for the conversion of CO_2 to bicarbonate (HCO_3^-). The *dabB* gene codes for a membrane protein that is implicated in establishing or utilizing a proton gradient, playing a role in the energy-dependent transport of inorganic carbon across the cell membrane. Together, the presence of *dabA* and *dabB* in CUBES01 distinguishes it from closely related strains commonly employed in microbial biotechnology, such as *H. bluephagenesis* TD01 (50) and *Halomonas boliviensis* LC1 (51), as well as another isolate from the GSL north arm, *Halomonas utahensis* DSM 3051 (52, 53). This particular gene, implicated in inorganic carbon transport, is common among autotrophs that also bear genes such as RuBisCO and/or carbonic anhydrase (35). Given that CUBES01's genome does not appear to comprise a full Calvin–Benson–Bassham cycle, the presence of these genes in CUBES01 would suggest alternative roles in bicarbonate provision for essential metabolic pathways or maintaining intracellular pH, which is connected to the metabolisms of alkaliphiles. It is also plausible that the strain lost these capabilities or that *dabA* and *dabB* were acquired through horizontal gene transfer. This logic is supported by the occurrence of two 100% identical copies of *dabA* located in both contigs.

Phenotype and physiology

The preference of *Halomonas* sp. CUBES01 for halophilic conditions is unsurprising, given that the isolate was first obtained from the north arm (Gunnison Bay) of the GSL where

the salinity is commonly between 27% and 29%, with the predominant ions being sodium and chloride (54). The strain's alkaliphily, however, is unexpected, given the surveyed pH around the point of the sample collection site is close to neutral (55–57). Nevertheless, the development of a minimal (i.e., chemically defined) growth medium, derived from the optimum cultivation conditions, enabled the characterization of the strain's growth on several carbon sources. Notably, the strain grew well on sucrose and glucose with similar biomass yield, while growing poorly on fructose, yielding significantly less biomass than on the other two sugars. This is surprising, given that sucrose is a disaccharide comprised of glucose and fructose. The reasons for this are unknown in the context of CUBES01 but often lie with the uptake mechanisms, which in many bacteria can be rather specific to certain sugars (58, 59). Of the non-sugar substrates, especially glycerol and acetate allowed high growth and PHB yields (60). While both can be derived from non-edible (waste) biomass, especially the latter is seen as a next-generation feedstock in terrestrial (61) as well as space bioprocess engineering (62–64). It is likely that the downstream entry of acetate into metabolism, which commonly proceeds via acetyl-CoA, stimulated PHB formation, as the pathway branches off directly from that intermediate. Also, amino sugars are of particular interest for this application, as these can be obtained from, e.g., cyanobacterial lysate via *in situ* resource utilization (65). Of these, the utilization of acetyl-glucosamine resulted in the highest PHB yield, which aligns with the finding that acetate enhances PHB production.

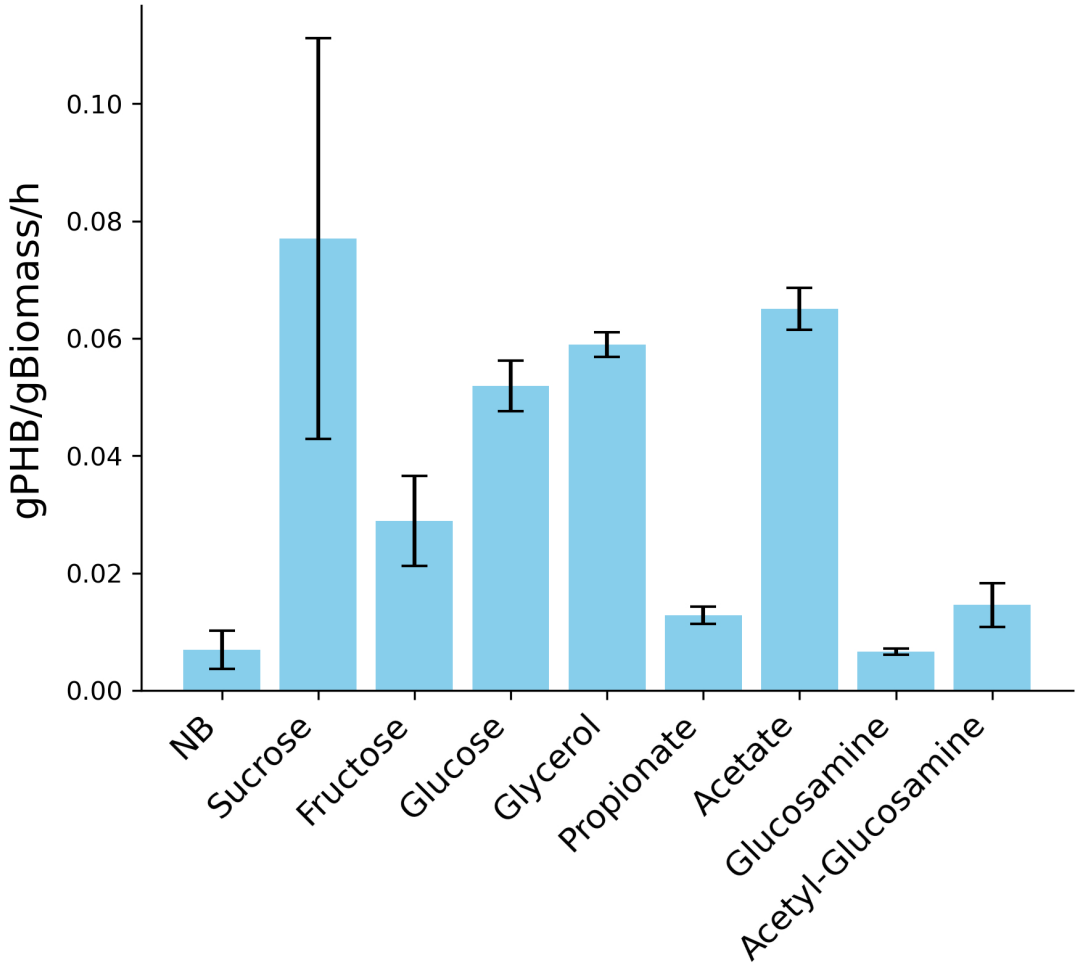

FIG 7 Estimated biomass-specific maximum PHB production rates of *Halomonas* sp. CUBES01. Data based on rates of biomass formation during exponential growth and PHB content during late exponential phase. Data correspond to values shown in Fig. 5 and 6.

During the cultivation of CUBES01 on various substrates, we observed a consistent pattern of pH changes, characterized by an initial drop followed by a subsequent rise to near-initial levels, except in the case of a complex substrate (Fig. 5). The sustained increase in pH observed with the complex substrate can be attributed to its non-buffered composition, which differs from the carbonate-buffered chemically defined medium. In the latter case, CUBES01 may have initially metabolized the respective carbon sources into organic acids, such as acetate and lactate, which were found in supernatant samples. The rise of the pH during the late exponential phase could be associated with a diauxic shift where the produced organic acids are consumed again (66). This is supported by the observation that with organic acids such as acetate and propionate as substrates, the final extracellular pH was slightly higher than with sugars or sugar alcohols.

Potential of PHB production

Interestingly, CUBES01 exhibited PHB production during both early and late growth phases, contrary to the conventional notion that PHB accumulation occurs under nutrient depletion or electron acceptor-deficient conditions (21, 67). This underscores the multifaceted role of PHA beyond being a mere storage product for energy and carbon, extending to encompass various stress response mechanisms. For instance, PHB production has been shown to confer salt stress resistance by preventing protein aggregation in halotolerant strains, such as *Pseudomonas* sp. CT13 (32). Furthermore, in *Halomonadaceae*, PHB production positively correlates with salinity (33). Another study of extreme halophiles has demonstrated the salinity threshold for halophiles' anabolic metabolisms to exceed the presently accepted limit dictated by cell division (68). This suggests that in halophiles, PHAs may serve additional functions beyond their role as an energy storage compound. Similarly, for thermophiles such as *Chelatococcus daeguensis* TAD1, elevated heat serves as a stress factor triggering PHB accumulation during growth (69), even in the absence of nutrient limitations.

Based on the maximum growth rate and an OD-to-biomass correlation (Table S8) that was obtained from samples collected during the late exponential growth phase of CUBES01 on different substrates, biomass-specific maximum PHB production rates were estimated (Fig. 7).

While the maximum overall achievable biomass concentration of CUBES01 was not specifically optimized, other *Halomonas* strains have reached maximum CDWs of 87.3, 80, and 44 g/L CDW [in the case of *Halomonas venusta* KT832796, *H. bluephagenesis* TD01, and *H. boliviensis* LC1, respectively (70–72)]. With an average of the reported biomass concentrations of 70.4 g/L, we deducted potential volumetric PHB production rates of 5.6, 3.5, 4.2, and 4.9 g_{PHB}/h for sucrose, glucose, glycerol, and acetate, respectively, based on the estimations shown in Fig. 7. These notably high projected rates suggest that CUBES01 holds great promise as a platform for bioplastics production.

Osmolytes and osmolysis

Given that *Halomonas* strains thrive in hyper- or moderately saline environments, they are likely to be susceptible to lysis when subjected to rapid change osmotic downshock. Taking advantage of this phenomenon could simplify the purification of bioplastic and reduce or even entirely abolish the need for organic solvents. Mechano-sensitive genes are pivotal for imparting resistance to changes in ionic strength, as evidenced by studies demonstrating improved osmolysis when knocked out, even of non-halophilic microorganisms (73). While such genes are also present in CUBES01 (*mscK* or *mscL*), they appear to be not preventing the osmolysis susceptibility of the strain. This opens the door to simplified and rapid purification of intracellular products, reducing process complexity and resource requirements.

Genetic tractability

The ability to transform CUBES01 with broad-host-range plasmid vectors through bacterial conjugation opens up the opportunity for genetic manipulation of the

strain, a rare capacity among *Halomonadaceae* (74). However, further characterization and development of genetic tools are needed before heterologous genes may be expressed or the genome of CUBES01 can be reliably modified. Poor growth of the transformed mutants bearing pCM66T was likely due to the alternate aminoglycoside 3′-phosphotransferase gene harbored by that plasmid [i.e., aph(3′)-II, while pBBR1MCS bears aph(3′)-Ia], presumably conveying insufficient antibiotic resistance. We note that aph(3′)-Ia is also frequently annotated as *aphA1* or *kanR* and *aph*, *nptII* or *neo*, respectively.

Conclusions

Extremophiles like *Halomonadaceae* bear great potential to make bio-manufacturing more economical, as they can reduce or abolish the need for aseptic process conditions to maintain a pure culture. In addition, the high ionic strength of the cultivation medium enables the release of intracellular products, such as bio-polyesters, via osmolysis, which could be a more cost-efficient and environmentally friendly method of downstream processing. Further, the finding that CUBES01 accumulated PHB predominantly during exponential growth is significant for industrial applications, due to the possibility for continuous process operation, increasing overall productivity. Paired with projected plausible productivities in the range of 5 g/h from different carbon sources on a minimal medium, this further enhances CUBES01's attractiveness for microbial biotechnology, improving process viability through reduced feedstock cost. The opportunity to simplify the release of the intracellular product brings sustainable production of bioplastics further into reach.

MATERIALS AND METHODS

Sampling and isolation of the *Halomonas* species

A 500-mL sample of water from the GSL in Utah was taken near the Spiral Jetty of Rozel Point at 41°26′15.5″N 112°40′09.7″W (see map in Fig. 1a) and kept refrigerated for transport. Upon arrival at the lab 48 h after collection, the sample was concentrated 33.3-fold by centrifuging at 4,816 × *g* for 20 minutes and re-suspension of the resulting pellet in 15 mL of the supernatant. One milliliter of the concentrated sample was used to inoculate liquid NB that contained 200 g/L (20% wt/vol) of sodium chloride. After 2 weeks of incubation at 30°C, 100 µL of the culture was spread on NB agar that contained 200 g/L of sodium chloride. The plates were incubated at 30°C for 2 weeks. The six colonies that appeared were transferred to fresh NB agar plates with 200 g/L sodium chloride. The individual isolates were preserved as glycerol stocks for further characterization.

Construction of pairwise genetic distance heatmap and phylogenetic tree

The 16S rRNA genes of the isolates were sequenced using bacterial 8F and 1492R primers as shown in Table S6. In addition to the near full-length (1,406 bp) nucleotide 16S rRNA sequence of CUBES01 (OQ359097.1), 49 16S rRNA sequences of related *Halomonas* species and 1 from *Zymobacter* (as an outer group) were derived from GenBank. The sequences were aligned and trimmed using Geneious by Dotmatics (Biomatters, Inc.) (75). Based on that, the pairwise distance heatmap and the phylogenetic tree were constructed using Python 3.12.2 and MEGA11 (76), respectively. In the phylogenetic tree, the evolutionary history was inferred using the minimum evolution method, and the evolutionary distances were computed using the maximum composite likelihood method.

Whole-genome sequencing, assembly, and annotation

Genome sequencing of the *Halomonas* species was performed by Plasmidsaurus, Eugene, OR, USA, using amplification-free long-read sequencing library preparation, utilizing Oxford Nanopore Technologies (ONT) v14 library prep chemistry. This approach was specifically chosen to ensure minimal fragmentation of the input gDNA, maintaining the integrity and continuity of the genomic sequences. A total of 570,942,477 bp was obtained across ~148k reads. The sequencing was performed using ONT's R10.4.1 flow cells without the use of primers. The sequencing data exhibited high quality, with the longest read being ~66 kb and coverage of 155×, thus providing a robust data set for assembly.

The genome assembly began with the removal of the bottom 5% lowest quality fastq reads via Filtlong v0.2.1 with default parameters. The reads were then downsampled by 250 Mb to create a rough sketch of the assembly with Miniasm v0.3 (77). Using information acquired from the Miniasm assembly, the reads were then re-downsampled to ~100× coverage with heavy weight applied to remove low-quality reads. Flye (78) v2.9.1 and Medaka v1.8.0 were then leveraged to assemble with parameters selected for high-quality ONT reads. The assembled genome had a coverage of 103× encompassing two contigs with a combined size of 3.7 Mb. A larger contig consisted of 3,641,888 bp, while a smaller contig with higher coverage consisted of 26,118 bp, part of which was identified to be a repeat of a section of the larger contig. Functional analysis and prediction of certain genes were conducted using InterPro 98.0 (79).

Gene annotation, conducted using the Department of Energy's KBase (80) and RASTtk v1.073 (81) using the B (Bacteria) domain default parameters, identified a feature count of 10,208 for the larger and 70 for the shorter contig. The genome analysis and characterization were based on the larger contig unless stated otherwise.

The annotated genome was imported into Pathway Tools software version 27.0 (82) where it was used to generate a pathway/genome database file using the PathoLogic (83) and MetaCyc version 27.0 (84). Pathway Tools was then leveraged to construct a comprehensive metabolic profile map (SI1).

Analysis of Codon Usage Bias

The CUB of CUBES01 was analyzed based on the assembled genome. The CUB values (frequency of codons) for each amino acid were assessed using the Jamie McGowan Bioinformatics Tools (85).

Admittance to and inclusion of *Halomonas* sp. CUBES01 in strain collections

The *Halomonas* strain was deposited to the *Deutsche Sammlung von Mikroorganismen und Zellkulturen* (DSMZ) GmbH at the Leibnitz Institute (Braunschweig, Germany) under the designation CUBES01 and is available under accession number DSM 115203. In addition, the following services and analyses were carried out by DSMZ: Production of Biomass in Quantified Aliquots for Special Procedures, as well as Analysis of Cellular Fatty Acids (Table S1), Analysis of Respiratory Quinones (Results), Analysis of Metabolic Activities (Table S2), and Antibiotic Susceptibility Testing (Table S3).

The *Halomonas* strain was also deposited to the Korean Collection for Type Cultures (KCTC) at the Korean Research Institute of Bioscience and Biotechnology (Daejeon, South Korea) under the designation CUBES01 and is available under accession number KCTC 92801.

Preparation of salinity and pH gradient agar

Gradient agar plates were produced using square culture/Petri dishes, analogously to previously described toxicity tests (65). More specifically, for salinity, two solutions of NB agar with different salt contents (i.e., no sodium chloride and 175 g/L of sodium chloride, Fig. S3) were used to sequentially pour two layers of solid medium on top of

each other at different angles. That way a horizontal gradient was achieved through the linear difference in vertical thickness of each individual layer. Gradient agar plates of pH were produced similarly with layers of NB agar, as per an established protocol (86), while the total concentration of ions was kept at 1 M for optimum growth conditions. The following buffers were used to maintain the boundaries of the two different pH-gradient plates: The lower and higher pH for a gradient from 7 to 9 (Fig. S4a) was achieved with a 100 mM phosphate buffer, using the respective required amounts of KH_2PO_4 and KH_2PO_4. The lower pH for the gradient from 6.6 to 10.2 (Fig. S4b) was obtained analogously, while the higher pH was reached using a 10 mM Tris buffer system. For the latter, 90 mL of Tris solution was titrated to pH 10.2 using a monovalent strong base. The volume was made up to 100 mL with pure water, achieving a final buffer concentration of 10 mM.

Cultivation of *Halomonas* sp. CUBES01

Unless stated otherwise, the strain was routinely maintained and propagated at 30°C on solid medium (agar plates) that contained 100 g/L sodium chloride with NB as the substrate. For growth experiments using liquid medium, to determine the maximum doubling time, as well as accumulate biomass for PHB production, *Halomonas* sp. CUBES01 was cultivated at 30°C in 500 mL baffled shake flasks (polycarbonate with vented screw cap) with 180 rpm shaking (culture volume maximum 10% of shake flask capacity). Unless stated otherwise, 1 M sodium chloride maintained optimum osmotic strength, e.g., when using Luria–Bertani (LB), NB, or a 1:1 mixture of both as substrate. The composition of the chemically defined (minimal) medium used to characterize the growth of *Halomonas* sp. CUBES01 on different substrates and determine the biomass and PHB yields, as well as analyze extracellular metabolites, is given in Table 2 while the composition of the respective stock solutions is provided in Table 3.

Observation of microbial growth and determination of rates

Microbial growth in liquid culture was monitored by determining the optical density at a wavelength of 600 nm (OD_{600}) using a DR2800 Portable Spectrophotometer (Hach). Culture samples were collected by centrifugation (4,480 × *g* for 20 minutes) to obtain supernatant for metabolite analysis and biomass for PHA extraction. Generally, experiments involving shake flask cultivation were performed in duplicates.

The growth rates μ were derived from the parameter k in the exponential growth model $y(t) = A\exp(-k \times t)$, where A is the initial amount of growth, k is the rate of growth (negative in the context of decay), and t is time. We represent growth rate μ as $\mu = -k$ to reflect a positive growth rate since a positive k typically indicates decay rather than growth. The standard deviation of μ, denoted as σ_μ, is equivalent to the standard deviation of k, which is derived from the covariance matrix cov returned by the curve fitting function curve_fit. The diagonal elements of cov provide the variance of each fitted parameter; hence, σ_k is the square root of the variance of k: $\sigma_\mu = \sigma_k$. The doubling time t_d was calculated from the growth rate k using the formula $t_d = \frac{-\ln(2)}{k}$. To calculate the standard deviation of t_d, denoted as σ_{t_d}, we apply the formula for the propagation of uncertainties when the function is dependent on one measured quantity $\sigma_{t_d} = \left|\frac{dt_d}{dk}\right| \times \sigma_k$. Taking the derivative of t_d with respect to k as $\frac{dt_d}{dk} = -\frac{\ln(2)}{k^2}$. Thus, the standard deviation of t_d is given by $\sigma_{t_d} = \frac{\ln(2)}{k^2} \times \sigma_k$.

PHA extraction and ^{1}H nuclear magnetic resonance spectroscopy

Bio-polyesters (PHAs) were recovered from freeze-dried cell-mass employing chloroform extraction (39). The weight of the recovered polymer was determined gravimetrically,

and the composition was analyzed employing NMR spectroscopy as previously reported (87): a few milligrams of polymer was dissolved in deuterated chloroform, and ^{1}H-NMR spectra were recorded at 25°C on a Unity INOVA 500 NMR Spectrometer (Varian Medical Systems) with chemical shifts referenced in parts per million relative to tetramethylsilane.

Gel permeation chromatography

GPC was carried out in chloroform on a TSKgel SuperHZM-H column (Tosoh) with a Dawn MultiAngle Light Scattering detector (Wyatt Technology) and an Optilab T-rEX differential refractometer (Wyatt Technology). Polystyrene calibrated (from $M_p = 500 - 275,000$ g/mol) molecular weights were determined using a GPCmax autosampler at 25°C at a flow rate of 1 mL/min.

High-performance liquid chromatography

The quantification of acetate and lactate in the culture broth was based on a previously published HPLC method for the detection of organic acids (88). Briefly, the procedure was as follows: Samples of 1 mL were filtered [polyvinylidene difluoride (PVDF) and polyethersulfone (PES) syringe filters, 0.2 µm pore size] and diluted 1:100 into HPLC sampling vials. Analysis of 50-µL sample volume was performed on a 1260 Infinity HPLC system (Agilent), using an Aminex HPX87H column (BioRad) with 5 mM H_2SO_4 as the eluent, at a flow rate of 0.7 mL/min. Organic acids were identified by their retention times and quantified by comparison to standards of known concentration using a refractive index detector operated at 35°C or a UV detector at 210 nm.

TABLE 3 Composition of stock solutions for chemically defined medium

Component	Amount (g/L)	Comments/Notes
Basic salts		
KNO_3	2	Prepare as 2× stock solution and autoclave at 121°C for 20 minutes. Let cool down before adding remaining components.
$MgSO_47H_2O$	0.4	
$CaCl_2H_2O$	0.04	
NaCl	116.88	
Trace elements		
Na_2EDTA	5	Prepare as 1,000× stock solution and autoclave at 121°C for 20 minutes. After autoclaving, the solution becomes pink.
$FeSO_47H_2O$	2	
$ZnSO_47H_2O$	0.3	
$MnCl_24H_2O$	0.03	
$CoCl_26H_2O$	0.2	
$CuSO_45H_2O$	1.2	
$Na_2O_4W2H_2O$	0.3	
$NiCl_26H_2O$	0.05	
$Na_2MoO_42H_2O$	0.05	
H_3BO_3	0.03	
Phosphate buffer (80 mM)		
KH_2PO_4	5.44	Prepare as 50× stock solution (total phosphate concentration of 80 mM) and autoclave at 121°C for 20 minutes; the pH of the solution should be between 6.8 and 7.
Na_2HPO_4	5.68	
Carbonate buffer (1 M)		
$NaHCO_3$	75.6	Prepare as 25× stock solution (total carbonate concentration of 1 M) and sterilize by filtration only; the pH of the solution should be between 8.6 and 9.
Na_2CO_3	10.5	
Carbon source		
Variable (sucrose, glucose, fructose, glycerol, glucosamine, acetate, acetyl-glucosamine)		Prepare suitable stock solutions (e.g., 10× or 20×) for desired concentration (e.g., 100 or 200 g/L). Sterilize by filtration only.

Microscopy and fluorescence staining of intracellular PHAs

Cells previously frozen in 20% glycerol were thawed on ice, and 10 µL was stained with 2 µL of a 10 µg/mL Nile red solution. Microscopy was performed on a Leica DM 4000 B epifluorescence microscope using an HCX PL APO 100× oil immersion objective with identical illumination and magnification settings for all images. Images were taken with a Leica DFC 500 camera and the Leica Application Suite V 3.8 software with identical settings for all images. Scale bars were added manually based on the camera software's information that one pixel represents 0.092 µm.

For the determination of the relative fluorescence intensity of the cell cultures, a Spark Multimode Microplate Reader (Tecan) was used. Samples previously collected from different growth stages were diluted to an approx. OD_{600} of 1 as applicable, and aliquots of 200 µL containing 0.0001% Nile red were distributed into a clear 96-well round-bottom microtiter plate, along with no-growth (media) blanks. The optical density and fluorescence were measured in four runs, using the following specific settings: absorbance at 600 nm wavelength with 10 flashes and 50 ms settle time across all runs. Fluorescence by monochromator (excitation and emission) across all runs:

- Bottom reading: 30 flashes (5 × 6 flashes per well), 40 µs integration time, 0 µs lag time, 0 ms settle time, Z-position of 26 mm with either
  - 530 nm excitation wavelength, 20 nm excitation bandwidth, 610 nm emission wavelength, 20 nm emission bandwidth, gain optimal of 109 or
  - 535 nm excitation wavelength, 10 nm excitation bandwidth, 610 nm emission wavelength, 20 nm emission bandwidth, gain optimal of 126
- Top reading: 30 flashes, automatic mirror (dichroic 560), 40 µs integration time, 0 µs lag time, 0 ms settle time, Z-position of 20 mm with either
  - 530 nm excitation wavelength, 20 nm excitation bandwidth, 610 nm emission wavelength, 20 nm emission bandwidth, gain optimal of 55 or
  - 535 nm excitation wavelength, 10 nm excitation bandwidth, 610 nm emission wavelength, 20 nm emission bandwidth, gain optimal of 80

The individual reads were calibrated to zero based on the recorded baseline absorbance of the respective blanks for each respective medium and run and normalized to the absorbance before averaging the reads of the samples of the four runs; the standard deviation of the samples was calculated for the biological replicates of the shake flask cultures.

Osmolysis susceptibility test

The lysis rate of CUBES01 when exposed to an osmotic shock was quantified as the change of optical density (OD_{600}) of a cell suspension over a short time. Cells from the exponential phase of shake flask culture on NB-saline medium (1 M of sodium chloride) were harvested by centrifugation (4,480 × *g* for 20 minutes) and resuspended in deionized water, while the OD was measured before the osmotic shock, as well as at 1, 10, 20, and 40 min thereafter. Further, CFU of the original culture as well as the cell suspension after the osmotic shock were determined by plating 100 µL of 10^4-fold dilutions, based on the initial OD_{600} (0.6) of the culture at the point of collection, which had an estimated cell count of ~4.7×10^7 cells/mL (89).

Transformation of CUBES01 by conjugation

The protocol for the transformation of *Halomonas* sp. CUBES01 was developed outgoing from an established method for plasmid vector mobilization by means of bacterial conjugation, with certain conditions adjusted in analogy to protocols for other halophiles (90), as outlined in the following. Specifically, the B2155 derivative *E. coli* strain WM3064 (*thrB1004 pro thi rpsL hsdS lacZ*ΔM15 RP4-1360 Δ(*araBAD*)567 Δ*dapA*1341::[*erm pir*]), an RP4 mobilizing *λpir* cell line that is auxotrophic for diaminopimelic acid (DAP),

was transformed with the respective plasmid vectors (pTJS140, pBBR1MCS, and pCM66T; see Table S5 for details) using the "Mix and Go!" *E. coli* Transformation Kit (Zymo Research, Irvine, CA).

The WM3064 strains bearing the respective plasmid vectors, hereafter referred to as the donor strains, were incubated at 30°C overnight on solid LB containing DAP (300 µM) and kanamycin (50 µg/mL) or streptomycin (50 µg/mL) as applicable, while the recipient strain, CUBES01, was incubated at 30°C overnight on solid NB with 1 M sodium chloride. From the agar plates, liquid cultures of the donor strains were inoculated on LB containing the respective antibiotic and DAP and incubated with shaking at 30°C overnight. Simultaneously, the recipient strain was inoculated in the liquid cultures of NB with 1 M sodium chloride, also incubated at 30°C overnight. On the next day, 6 µL of the donor strain culture was used to inoculate 3 mL of fresh LB containing DAP and 35 g/L of sodium chloride (no antibiotics). Likewise, 20 µL of the recipient strain was used to inoculate 10 mL of fresh NB containing 35 g/L of sodium chloride. Both cultures were incubated with shaking at 30°C. After 4 h, the two liquid cultures (3 mL of the donor strain and 10 mL of the recipient strain) were combined, and the cells were collected by centrifugation (10 minutes at 4,816 × *g*). The supernatant was discarded, and the cells were resuspended in the remaining liquid. The cell suspension was pipetted as a drop on a prewarmed NB plate containing DAP and 35 g/L sodium chloride and incubated at 30°C overnight with the plate facing up. On the next day, the biomass was collected and suspended in 500 µL of NB that contained 1 M of sodium chloride. Aliquots of the cell suspension were diluted 1:10 and 1:100, and volumes of 100–200 µL of all three concentrations (original suspension and two dilutions) were plated on NB that contained 1 M sodium chloride and the appropriate antibiotic for the respective plasmid vector. The plates were incubated at 30°C, and single colonies that appeared after 1–2 days were isolated on the same type of solid medium for screening purposes.

Validation of transformed CUBES01

DNA was purified from the antibiotic-resistant mutants of *Halomonas* sp. CUBES01 using a Plasmid Mini Kit (Qiagen, Hilden, Germany) for screening the presence of the respective plasmids. The amplicons indicative of the shuttle vectors were obtained from PCRs targeting complementary regions of the respective plasmids: two primer sets were used per plasmid; (i) araC (forward) and spc (reverse) and (ii) spc (forward) and araC (reverse) were used to confirm the presence of pTJS140; (i) neoR (forward) and araC (reverse) and (ii) araC (forward) and neoR (reverse) were used to confirm the presence of pBBR1MCS.

ACKNOWLEDGMENTS

This work was partially supported by the National Aeronautics and Space Administration (NASA) under grant or cooperative agreement award numbers NNX17AJ31G and 80NSSC22K1474. Any opinions, findings, conclusions, or recommendations expressed in this material are those of the author and do not necessarily reflect the views of NASA.

AUTHOR AFFILIATIONS

[1]Center for the Utilization of Biological Engineering in Space (CUBES), Berkeley, California, USA
[2]Department of Civil and Environmental Engineering, Stanford University, Stanford, California, USA
[3]Department of Bioengineering, University of California, Berkeley, California, USA
[4]Department of Chemistry, Stanford University, Stanford, California, USA

AUTHOR ORCIDs

Sung-Geun Woo http://orcid.org/0000-0002-1941-2086
Nils J. H. Averesch http://orcid.org/0000-0002-6389-2646

Aaron J. Berliner http://orcid.org/0000-0002-4817-3926
Joerg S. Deutzmann http://orcid.org/0000-0002-1337-4103

FUNDING

Funder	Grant(s)	Author(s)
National Aeronautics and Space Administration (NASA)	NNX17AJ31G, 80NSSC22K1474	Sung-Geun Woo Nils J. H. Averesch Craig S. Criddle
National Aeronautics and Space Administration (NASA)	NNX17AJ31G	Aaron J. Berliner Vince E. Payne

DATA AVAILABILITY

The sequenced genome of *Halomonas* sp. CUBES01 was deposited to the GenBank database under accession number ASM2099100v2. The GenBank accession number for the 16S rRNA gene sequence of CUBES01 is OQ359097.1. All other data and code are freely accessible as a GitHub repository.

ADDITIONAL FILES

The following material is available online.

Supplemental Material

File SI1 (AEM00603-24-s0001.pdf). Metabolic map of *Halomonas* sp. CUBES01.
File SI2 (AEM00603-24-s0002.zip). Microscopy images of *Halomonas* sp. CUBES01.
Supplemental material (AEM00603-24-s0003.pdf). Tables S1 to S9; Fig. S1 to S9.

REFERENCES

1. Geyer R, Jambeck JR, Law KL. 2017. Production, use, and fate of all plastics ever made. Sci Adv 3:e1700782. https://doi.org/10.1126/sciadv.1700782
2. Nicholson SR, Rorrer NA, Carpenter AC, Beckham GT. 2021. Manufacturing energy and greenhouse gas emissions associated with plastics consumption. Joule 5:673–686. https://doi.org/10.1016/j.joule.2020.12.027
3. Smith J, Vignieri S. 2021. A devil's bargain. Science 373:34–35. https://doi.org/10.1126/science.abj9099
4. US EPA. 2020. Advancing sustainable materials management: 2018 tables and figures. Technical report. Washington, DC United States Environmental Protection Agency. https://www.epa.gov/sites/default/files/2021-01/documents/2018_tables_and_figures_dec_2020_fnl_508.pdf.
5. PlasticsEurope (PEMRG). 2022. Annual production of plastics worldwide from 1950 to 2021. Available from: https://www.statista.com/statistics/282732/global-production-of-plastics-since-1950
6. Alex Tullo. 2023. Bulking up polyester recycling. C&EN Global Enterp 101:20–26. https://doi.org/10.1021/cen-10139-cover
7. Main D. 2023. Think that your plastic is being recycled? Think again. MIT Technology Review. https://www.technologyreview.com/2023/10/12/1081129/plastic-recycling-climate-change-microplastics.
8. Meier MAR, Metzger JO, Schubert US. 2007. Plant oil renewable resources as green alternatives in polymer science. Chem Soc Rev 36:1788–1802. https://doi.org/10.1039/b703294c
9. Brandon AM, Criddle CS. 2019. Can biotechnology turn the tide on plastics? Curr Opin Biotechnol 57:160–166. https://doi.org/10.1016/j.copbio.2019.03.020
10. Tsang YF, Kumar V, Samadar P, Yang Y, Lee J, Ok YS, Song H, Kim K-H, Kwon EE, Jeon YJ. 2019. Production of bioplastic through food waste valorization. Environ Int 127:625–644. https://doi.org/10.1016/j.envint.2019.03.076
11. Guerrero-Cruz S, Vaksmaa A, Horn MA, Niemann H, Pijuan M, Ho A. 2021. Methanotrophs: discoveries, environmental relevance, and a perspective on current and future applications. Front Microbiol 12:678057. https://doi.org/10.3389/fmicb.2021.678057
12. Lu H, Zhang G, He S, Zhao R, Zhu D. 2021. Purple non-sulfur bacteria technology: a promising and potential approach for wastewater treatment and bioresources recovery. World J Microbiol Biotechnol 37:161. https://doi.org/10.1007/s11274-021-03133-z
13. Nanda N, Bharadvaja N. 2022. Algal bioplastics: current market trends and technical aspects. Clean Technol Environ Policy 24:2659–2679. https://doi.org/10.1007/s10098-022-02353-7
14. Choi SY, Park SJ, Kim WJ, Yang JE, Lee H, Shin J, Lee SY. 2016. One-step fermentative production of poly(lactate-*co*-glycolate) from carbohydrates in *Escherichia coli*. Nat Biotechnol 34:435–440. https://doi.org/10.1038/nbt.3485
15. Chen G-Q, Jiang X-R, Guo Y. 2016. Synthetic biology of microbes synthesizing polyhydroxyalkanoates (PHA). Synth Syst Biotechnol 1:236–242. https://doi.org/10.1016/j.synbio.2016.09.006
16. Yang JE, Park SJ, Kim WJ, Kim HJ, Kim BJ, Lee H, Shin J, Lee SY. 2018. One-step fermentative production of aromatic polyesters from glucose by metabolically engineered *Escherichia coli* strains. Nat Commun 9:79. https://doi.org/10.1038/s41467-017-02498-w
17. Mannina G, Presti D, Montiel-Jarillo G, Carrera J, Suárez-Ojeda ME. 2020. Recovery of polyhydroxyalkanoates (PHAs) from wastewater: a review. Bioresour Technol 297:122478. https://doi.org/10.1016/j.biortech.2019.122478
18. Sirohi R, Prakash Pandey J, Kumar Gaur V, Gnansounou E, Sindhu R. 2020. Critical overview of biomass feedstocks as sustainable substrates for the production of polyhydroxybutyrate (PHB). Bioresour Technol 311:123536. https://doi.org/10.1016/j.biortech.2020.123536
19. Matos M, Cruz RAP, Cardoso P, Silva F, Freitas EB, Carvalho G, Reis MAM. 2021. Combined strategies to boost polyhydroxyalkanoate production

from fruit waste in a three-stage pilot plant. ACS Sustainable Chem Eng 9:8270–8279. https://doi.org/10.1021/acssuschemeng.1c02432
20. Andhalkar VV, Foong SY, Kee SH, Lam SS, Chan YH, Djellabi R, Bhubalan K, Medina F, Constantí M. 2023. Integrated biorefinery design with techno-economic and life cycle assessment tools in polyhydroxyalkanoates processing. Macro Materials & Eng 308:2300100. https://doi.org/10.1002/mame.202300100
21. Mitra R, Xu T, Xiang H, Han J. 2020. Current developments on polyhydroxyalkanoates synthesis by using halophiles as a promising cell factory. Microb Cell Fact 19:86. https://doi.org/10.1186/s12934-020-01342-z
22. Steinbüchel A. 2001. Perspectives for biotechnological production and utilization of biopolymers: metabolic engineering of polyhydroxyalkanoate biosynthesis pathways as a successful example. Macromol Biosci 1:1–24. https://doi.org/10.1002/1616-5195(200101)1:1<1::AID-MABI1>3.0.CO;2-B
23. Ye J, Hu D, Che X, Jiang X, Li T, Chen J, Zhang HM, Chen G-Q. 2018. Engineering of *Halomonas bluephagenesis* for low cost production of poly(3-hydroxybutyrate-*co*-4-hydroxybutyrate) from glucose. Metab Eng 47:143–152. https://doi.org/10.1016/j.ymben.2018.03.013
24. Biswas J, Jana SK, Mandal S. 2022. Biotechnological impacts of *Halomonas*: a promising cell factory for industrially relevant biomolecules. Biotechnol Genet Eng Rev 17:1–30. https://doi.org/10.1080/02648725.2022.2131961
25. Ling C, Qiao G-Q, Shuai B-W, Olavarria K, Yin J, Xiang R-J, Song K-N, Shen Y-H, Guo Y, Chen G-Q. 2018. Engineering NADH/NAD^+ ratio in *Halomonas bluephagenesis* for enhanced production of polyhydroxyalkanoates (PHA). Metab Eng 49:275–286. https://doi.org/10.1016/j.ymben.2018.09.007
26. Rathi D-N, Amir HG, Abed RMM, Kosugi A, Arai T, Sulaiman O, Hashim R, Sudesh K. 2013. Polyhydroxyalkanoate biosynthesis and simplified polymer recovery by a novel moderately halophilic bacterium isolated from hypersaline microbial mats. J Appl Microbiol 114:384–395. https://doi.org/10.1111/jam.12083
27. Quillaguamán J, Guzmán H, Van-Thuoc D, Hatti-Kaul R. 2010. Synthesis and production of polyhydroxyalkanoates by halophiles: current potential and future prospects. Appl Microbiol Biotechnol 85:1687–1696. https://doi.org/10.1007/s00253-009-2397-6
28. Jorge CD, Borges N, Bagyan I, Bilstein A, Santos H. 2016. Potential applications of stress solutes from extremophiles in protein folding diseases and healthcare. Extremophiles 20:251–259. https://doi.org/10.1007/s00792-016-0828-8
29. Becker J, Wittmann C. 2020. Microbial production of extremolytes – high-value active ingredients for nutrition, health care, and well-being. Curr Opin Biotechnol 65:118–128. https://doi.org/10.1016/j.copbio.2020.02.010
30. Ma H, Zhao Y, Huang W, Zhang L, Wu F, Ye J, Chen G-Q. 2020. Rational flux-tuning of *Halomonas bluephagenesis* for co-production of bioplastic PHB and ectoine. Nat Commun 11:3313. https://doi.org/10.1038/s41467-020-17223-3
31. Obulisamy PK, Mehariya S. 2021. Polyhydroxyalkanoates from extremophiles: a review. Bioresour Technol 325:124653. https://doi.org/10.1016/j.biortech.2020.124653
32. Soto G, Setten L, Lisi C, Maurelis C, Mozzicafreddo M, Cuccioloni M, Angeletti M, Ayub ND. 2012. Hydroxybutyrate prevents protein aggregation in the halotolerant bacterium *Pseudomonas* sp. CT13 under abiotic stress. Extremophiles 16:455–462. https://doi.org/10.1007/s00792-012-0445-0
33. Yoo Y, Young Kwon D, Jeon M, Lee J, Kwon H, Lee D, Seong Khim J, Choi Y-E, Kim J-J. 2024. Enhancing poly(3-hydroxybutyrate) production in halophilic bacteria through improved salt tolerance. Bioresour Technol 394:130175. https://doi.org/10.1016/j.biortech.2023.130175
34. Kim J, Kim Y-J, Choi SY, Lee SY, Kim K-J. 2017. Crystal structure of *Ralstonia eutropha* polyhydroxyalkanoate synthase C-terminal domain and reaction mechanisms. Biotechnol J 12. https://doi.org/10.1002/biot.201600648
35. Desmarais JJ, Flamholz AI, Blikstad C, Dugan EJ, Laughlin TG, Oltrogge LM, Chen AW, Wetmore K, Diamond S, Wang JY, Savage DF. 2019. DABs are inorganic carbon pumps found throughout prokaryotic phyla. Nat Microbiol 4:2204–2215. https://doi.org/10.1038/s41564-019-0520-8
36. Price GD, Long BM, Förster B. 2019. Dabs accumulate bicarbonate. Nat Microbiol 4:2029–2030. https://doi.org/10.1038/s41564-019-0629-9
37. Vreeland RH, Hochstein LI, eds. 1993. The biology of halophilic bacteria. CRC Press, Boca Raton, Florida.
38. Ma Y, Galinski EA, Grant WD, Oren A, Ventosa A. 2010. Halophiles 2010: life in saline environments. Appl Environ Microbiol 76:6971–6981. https://doi.org/10.1128/AEM.01868-10
39. Jacquel N, Lo C-W, Wei Y-H, Wu H-S, Wang SS. 2008. Isolation and purification of bacterial poly(3-hydroxyalkanoates). Biochem Eng J 39:15–27. https://doi.org/10.1016/j.bej.2007.11.029
40. Jain A, Srivastava P. 2013. Broad host range plasmids. FEMS Microbiol Lett 348:87–96. https://doi.org/10.1111/1574-6968.12241
41. Kim KK, Jin L, Yang HC, Lee S-T. 2007. *Halomonas gomseomensis* sp. nov., *Halomonas janggokensis* sp. nov., *Halomonas salaria* sp. nov. and *Halomonas denitrificans* sp. nov., moderately halophilic bacteria isolated from saline water. Int J Syst Evol Microbiol 57:675–681. https://doi.org/10.1099/ijs.0.64767-0
42. Wang T, Wei X, Xin Y, Zhuang J, Shan S, Zhang J. 2016. *Halomonas lutescens* sp. nov., a halophilic bacterium isolated from a lake sediment. Int J Syst Evol Microbiol 66:4697–4704. https://doi.org/10.1099/ijsem.0.001413
43. Baxter BK, Butler JK, eds. 2020. Great Salt Lake biology: a terminal lake in a time of change. Springer International Publishing, Cham.
44. Ramezani M, Pourmohyadini M, Nikou MM, Makzum S, Schumann P, Clermont D, Criscuolo A, Amoozegar MA, Kämpfer P, Spröer C. 2020. *Halomonas lysinitropha* sp. nov., a novel halophilic bacterium isolated from a hypersaline wetland. Int J Syst Evol Microbiol 70:6098–6105. https://doi.org/10.1099/ijsem.0.004504
45. Cai L, Tan D, Aibaidula G, Dong X-R, Chen J-C, Tian W-D, Chen G-Q. 2011. Comparative genomics study of polyhydroxyalkanoates (PHA) and ectoine relevant genes from *Halomonas* sp. TD01 revealed extensive horizontal gene transfer events and co-evolutionary relationships. Microb Cell Fact 10:88. https://doi.org/10.1186/1475-2859-10-88
46. Mitra R, Xu T, Chen G-Q, Xiang H, Han J. 2022. An updated overview on the regulatory circuits of polyhydroxyalkanoates synthesis. Microb Biotechnol 15:1446–1470. https://doi.org/10.1111/1751-7915.13915
47. Zher Neoh S, Fey Chek M, Tiang Tan H, Linares-Pastén JA, Nandakumar A, Hakoshima T, Sudesh K. 2022. Polyhydroxyalkanoate synthase (PhaC): the key enzyme for biopolyester synthesis. Curr Res Biotechnol 4:87–101. https://doi.org/10.1016/j.crbiot.2022.01.002
48. Maehara A, Taguchi S, Nishiyama T, Yamane T, Doi Y. 2002. A repressor protein, PhaR, regulates polyhydroxyalkanoate (PHA) synthesis via its direct interaction with PHA. J Bacteriol 184:3992–4002. https://doi.org/10.1128/JB.184.14.3992-4002.2002
49. Cai S, Cai L, Zhao D, Liu G, Han J, Zhou J, Xiang H. 2015. A novel DNA-binding protein, PhaR, plays a central role in the regulation of polyhydroxyalkanoate accumulation and granule formation in the haloarchaeon *Haloferax mediterranei*. Appl Environ Microbiol 81:373–385. https://doi.org/10.1128/AEM.02878-14
50. Chen X, Yin J, Ye J, Zhang H, Che X, Ma Y, Li M, Wu L-P, Chen G-Q. 2017. Engineering *Halomonas bluephagenesis* TD01 for non-sterile production of poly(3-hydroxybutyrate-*co*-4-hydroxybutyrate). Bioresour Technol 244:534–541. https://doi.org/10.1016/j.biortech.2017.07.149
51. Van-Thuoc D, Quillaguamán J, Mamo G, Mattiasson B. 2008. Utilization of agricultural residues for poly(3-hydroxybutyrate) production by *Halomonas boliviensis* LC1. J Appl Microbiol 104:420–428. https://doi.org/10.1111/j.1365-2672.2007.03553.x
52. Fendrich C. 1988. *Halovibrio variabilis* gen. nov. sp. nov., *Pseudomonas halophila* sp. nov. and a new halophilic aerobic Coccoid Eubacterium from Great Salt Lake, Utah, USA. Syst Appl Microbiol 11:36–43. https://doi.org/10.1016/S0723-2020(88)80046-8
53. Sorokin Dy, Tindall BJ. 2006. The status of the genus name *Halovibrio* Fendrich 1989 and the identity of the strains *Pseudomonas halophila* DSM 3050 and *Halomonas variabilis* DSM 3051. Request for an opinion. Int J Syst Evol Microbiol 56:487–489. https://doi.org/10.1099/ijs.0.63965-0
54. Jim Davis J, Gwynn W, Rupke A. 2022. Technical report. Commonly asked questions about Utah's Great Salt Lake and ancient Lake Bonneville. Utah Geological Survey.
55. Post FJ. 1977. The microbial ecology of the Great Salt Lake. Microb Ecol 3:143–165. https://doi.org/10.1007/BF02010403

56. Rupke A, Boden T. 2016. Survey notes. Vol. 48. Utah geological survey. https://geology.utah.gov/map-pub/survey-notes/salt-crust-great-salt-lake.
57. Jagniecki E, Rupke A, Kirby S, Nkenbrandt Pl. 2021. Technical report. Salt crust, brine, and marginal groundwater of Great Salt Lake's North Arm (2019 To 2021). Utah Geological Survey.
58. Deutscher J, Francke C, Postma PW. 2006. How phosphotransferase system-related protein phosphorylation regulates carbohydrate metabolism in bacteria. Microbiol Mol Biol Rev 70:939–1031. https://doi.org/10.1128/MMBR.00024-06
59. Deutscher J, Aké FMD, Derkaoui M, Zébré AC, Cao TN, Bouraoui H, Kentache T, Mokhtari A, Milohanic E, Joyet P. 2014. The bacterial phosphoenolpyruvate:carbohydrate phosphotransferase system: regulation by protein phosphorylation and phosphorylation-dependent protein-protein interactions. Microbiol Mol Biol Rev 78:231–256. https://doi.org/10.1128/MMBR.00001-14
60. Aytar Celik P, Barut D, Enuh BM, Erdogan Gover K, Nural Yaman B, Burcin Mutlu M, Cabuk A. 2023. A novel higher polyhydroxybutyrate producer *Halomonas halmophila* 18H with unique cell factory attributes. Bioresour Technol 372:128669. https://doi.org/10.1016/j.biortech.2023.128669
61. Kiefer D, Merkel M, Lilge L, Henkel M, Hausmann R. 2021. From acetate to bio-based products: underexploited potential for industrial biotechnology. Trends Biotechnol 39:397–411. https://doi.org/10.1016/j.tibtech.2020.09.004
62. Cestellos-Blanco S, Friedline S, Sander KB, Abel AJ, Kim JM, Clark DS, Arkin AP, Yang P. 2021. Production of PHB from CO_2-derived acetate with minimal processing assessed for space biomanufacturing. Front Microbiol 12:700010. https://doi.org/10.3389/fmicb.2021.700010
63. Averesch NJH. 2021. Choice of microbial system for *in-situ* resource utilization on Mars. Front Astron Space Sci 8:700370. https://doi.org/10.3389/fspas.2021.700370
64. Berliner AJ, Hilzinger JM, Abel AJ, McNulty MJ, Makrygiorgos G, Averesch NJH, Sen Gupta S, Benvenuti A, Caddell DF, Cestellos-Blanco S, et al. 2021. Towards a biomanufactory on Mars. Front Astron Space Sci 8:711550. https://doi.org/10.3389/fspas.2021.711550
65. Averesch NJH, Rothschild LJ. 2019. Metabolic engineering of *Bacillus subtilis* for production of *para* -aminobenzoic acid - unexpected importance of carbon source is an advantage for space application. Microb Biotechnol 12:703–714. https://doi.org/10.1111/1751-7915.13403
66. Wang X, Xia K, Yang X, Tang C. 2019. Growth strategy of microbes on mixed carbon sources. Nat Commun 10:1279. https://doi.org/10.1038/s41467-019-09261-3
67. Zhang L, Jiang Z, Tsui T-H, Loh K-C, Dai Y, Tong YW. 2022. A review on enhancing *Cupriavidus necator* fermentation for poly(3-hydroxybutyrate) (PHB) production from low-cost carbon sources. Front Bioeng Biotechnol 10:946085. https://doi.org/10.3389/fbioe.2022.946085
68. Paris ER, Arandia-Gorostidi N, Klempay B, Bowman JS, Pontefract A, Elbon CE, Glass JB, Ingall ED, Doran PT, Som SM, Schmidt BE, Dekas AE. 2023. Single-cell analysis in hypersaline brines predicts a water-activity limit of microbial anabolic activity. Sci Adv 9:eadj3594. https://doi.org/10.1126/sciadv.adj3594
69. Xu F, Huang S, Liu Y, Zhang Y, Chen S. 2014. Comparative study on the production of poly(3-hydroxybutyrate) by thermophilic *Chelatococcus daeguensis* TAD1: a good candidate for large-scale production. Appl Microbiol Biotechnol 98:3965–3974. https://doi.org/10.1007/s00253-014-5524-y
70. Stanley A, Punil Kumar HN, Mutturi S, Vijayendra SVN. 2018. Fed-batch strategies for production of PHA using a native isolate of *Halomonas venusta* KT832796 strain. Appl Biochem Biotechnol 184:935–952. https://doi.org/10.1007/s12010-017-2601-6
71. Quillaguamán J, Doan-Van T, Guzmán H, Guzmán D, Martín J, Everest A, Hatti-Kaul R. 2008. Poly(3-hydroxybutyrate) production by *Halomonas boliviensis* in fed-batch culture. Appl Microbiol Biotechnol 78:227–232. https://doi.org/10.1007/s00253-007-1297-x
72. Tan D, Xue Y-S, Aibaidula G, Chen G-Q. 2011. Unsterile and continuous production of polyhydroxybutyrate by *Halomonas* TD01. Bioresour Technol 102:8130–8136. https://doi.org/10.1016/j.biortech.2011.05.068
73. Adams JD, Sander KB, Criddle CS, Arkin AP, Clark DS. 2023. Engineering osmolysis susceptibility in *Cupriavidus necator* and *Escherichia coli* for recovery of intracellular products. Microb Cell Fact 22:69. https://doi.org/10.1186/s12934-023-02064-8
74. Fu X-Z, Tan D, Aibaidula G, Wu Q, Chen J-C, Chen G-Q. 2014. Development of *Halomonas* TD01 as a host for open production of chemicals. Metab Eng 23:78–91. https://doi.org/10.1016/j.ymben.2014.02.006
75. Kearse M, Moir R, Wilson A, Stones-Havas S, Cheung M, Sturrock S, Buxton S, Cooper A, Markowitz S, Duran C, Thierer T, Ashton B, Meintjes P, Drummond A. 2012. Geneious Basic: an integrated and extendable desktop software platform for the organization and analysis of sequence data. Bioinformatics 28:1647–1649. https://doi.org/10.1093/bioinformatics/bts199
76. Tamura K, Stecher G, Kumar S. 2021. MEGA11: molecular evolutionary genetics analysis version 11. Mol Biol Evol 38:3022–3027. https://doi.org/10.1093/molbev/msab120
77. Li H. 2016. Minimap and miniasm: fast mapping and *de novo* assembly for noisy long sequences. Bioinformatics 32:2103–2110. https://doi.org/10.1093/bioinformatics/btw152
78. Kolmogorov M, Yuan J, Lin Y, Pevzner PA. 2019. Assembly of long, error-prone reads using repeat graphs. Nat Biotechnol 37:540–546. https://doi.org/10.1038/s41587-019-0072-8
79. Paysan-Lafosse T, Blum M, Chuguransky S, Grego T, Pinto BL, Salazar GA, Bileschi ML, Bork P, Bridge A, Colwell L, et al. 2023. InterPro in 2022. Nucleic Acids Res 51:D418–D427. https://doi.org/10.1093/nar/gkac993
80. Arkin AP, Cottingham RW, Henry CS, Harris NL, Stevens RL, Maslov S, Dehal P, Ware D, Perez F, Canon S, et al. 2018. KBase: the United States department of energy systems biology knowledgebase. Nat Biotechnol 36:566–569. https://doi.org/10.1038/nbt.4163
81. Brettin T, Davis JJ, Disz T, Edwards RA, Gerdes S, Olsen GJ, Olson R, Overbeek R, Parrello B, Pusch GD, Shukla M, Thomason JA, Stevens R, Vonstein V, Wattam AR, Xia F. 2015. RASTtk: a modular and extensible implementation of the RAST algorithm for building custom annotation pipelines and annotating batches of genomes. Sci Rep 5:8365. https://doi.org/10.1038/srep08365
82. Karp PD, Paley S, Krummenacker M, Kothari A, Wannemuehler MJ, Phillips GJ. 2022. Pathway tools management of pathway/genome data for microbial communities. Front Bioinform 2:869150. https://doi.org/10.3389/fbinf.2022.869150
83. Karp PD, Latendresse M, Paley SM, Krummenacker M, Ong QD, Billington R, Kothari A, Weaver D, Lee T, Subhraveti P, Spaulding A, Fulcher C, Keseler IM, Caspi R. 2016. Pathway Tools version 19.0 update: software for pathway/genome informatics and systems biology. Brief Bioinform 17:877–890. https://doi.org/10.1093/bib/bbv079
84. Caspi R, Billington R, Fulcher CA, Keseler IM, Kothari A, Krummenacker M, Latendresse M, Midford PE, Ong Q, Ong WK, Paley S, Subhraveti P, Karp PD. 2018. The MetaCyc database of metabolic pathways and enzymes. Nucleic Acids Res 46:D633–D639. https://doi.org/10.1093/nar/gkx935
85. Stothard P. 2000. The sequence manipulation suite: JavaScript programs for analyzing and formatting protein and DNA sequences. Biotechniques 28:1102–1104. https://doi.org/10.2144/00286ir01
86. Sacks LE. 1956. A pH gradient agar plate. Nature 178:269–270. https://doi.org/10.1038/178269a0
87. Myung J, Wang Z, Yuan T, Zhang P, Van Nostrand JD, Zhou J, Criddle CS. 2015. Production of nitrous oxide from nitrite in stable type II methanotrophic enrichments. Environ Sci Technol 49:10969–10975. https://doi.org/10.1021/acs.est.5b03385
88. Lohner ST, Deutzmann JS, Logan BE, Leigh J, Spormann AM. 2014. Hydrogenase-independent uptake and metabolism of electrons by the archaeon *Methanococcus maripaludis*. ISME J 8:1673–1681. https://doi.org/10.1038/ismej.2014.82
89. Mira P, Yeh P, Hall BG. 2022. Estimating microbial population data from optical density. PLoS ONE 17:e0276040. https://doi.org/10.1371/journal.pone.0276040
90. Puri AW, Owen S, Chu F, Chavkin T, Beck DAC, Kalyuzhnaya MG, Lidstrom ME. 2015. Genetic tools for the industrially promising methanotroph *Methylomicrobium buryatense*. Appl Environ Microbiol 81:1775–1781. https://doi.org/10.1128/AEM.03795-14